JOURNAL OF COMPUTATIONAL PHYSICS 104, 313–320 (1993)

Numerical Calculation of the Equation of Flow in Porous Media: The Lattice Gas Approach

PAUL PAPATZACOS

Høgskolesenteret i Rogaland, Stavanger, Norway

Received July 13, 1990; revised August 7, 1991

Lattice gasses are models of gasses where the particles move in discretized space and time. A lattice gas model is defined by a lattice and a set of rules defining particle movements. The hydrodynamical equations of the gas are then found as successive terms in a perturbation expansion of the lattice Boltzmann equations. A lattice gas has been introduced in a previous publication, where it was shown that the lowest order term in the above-named expansion is the equation of one-phase flow in a homogeneous porous medium with two independent permeability components. The model assumes that the lattice gas density, as characterized by a density scale, is small. This paper presents a generalization to inhomogenous media with three independent permeability components. The main contribution of the paper is, however, a calculation of the flow equation of the lattice gas to the next order in the perturbation expansion of the Boltzmann equations, showing that correction terms proportional to the gas density appear in the permeability coefficients. A numerical example is given, in a case where the exact solution is known. The numerical results contain errors due to statistical fluctuations and deviations due to the correction terms mentioned above. For the particular example, the relative deviations are shown to be in the neighborhood of 5% for a 600 × 600 lattice and a density scale of about 0.1. © 1993 Academic Press, Inc.

1. INTRODUCTION

A lattice-gas model for the simulation of the equation of flow in a porous medium has recently been presented [4]. It consists of a lattice and of a set of rules, chosen in such a way that the density of the resulting lattice gas satisfies the differential equation of one-phase flow in a porous medium. The method of solution consists simply in measuring the density of the particles at a given place and a given time-step.

The porous medium simulated in [4] is homogeneous—all parameters are space independent—and slightly anisotropic—the permeability tensor is diagonal, with two independent components. The present paper has two main goals. The first is to introduce some generalizations that make it possible to simulate a porous medium which is not homogeneous and which has a diagonal permeability tensor with three independent components. The second is related to an essential assumption underlying the lattice gas model of [4], namely that of low density. Indeed, the differential equation governing the flow of this gas is obtained as the lowest order in a perturbation expansion of the lattice Boltzmann equations, where the expansion parameter is, effectively, the density. It is consequently important to be able to estimate the error attached to a given, necessarily finite, value of the density. This is done by getting the equation of motion which results from the inclusion of the next-to-lowest order in the perturbation expansion of the Boltzmann equations, thus making explicit the first terms that are neglected by the lowest order approximation.

The flow equation for an inhomogeneous and anisotropic porous medium is derived in Section 2, thus establishing the equation that one wishes to simulate. The lattice gas model itself is presented in Section 3, with the necessary generalizations to the model of [4]. The resulting Boltzmann equations and their perturbation solution are given in Section 4. Finally, in Section 5, the lattice gas method is applied to a specific problem with a known analytical solution. The deviations of the numerical results from the exact solution are estimated for a given scale of the density.

2. FLOW EQUATION FOR INHOMOGENEOUS, ANISOTROPIC POROUS MEDIA

The equation of one-phase flow in porous media, derived in [4] in the framework of continuum mechanics for the homogeneous case, is here generalized to the inhomogeneous and anisotropic case. To conform with the notation of the rest of this paper, space coordinates are denoted by (x'_1, x'_2, x'_3) and time is denoted by t'. A right-handed coordinate system is assumed, with the x'_2 axis pointing upwards [4]. Partial differentiation with respect to x'_i is sometimes denoted by ∂'_i and partial differentiation with respect to t' by ∂'_t. The summation convention is used for Latin indexes.

The flow equation can be derived by combining the mass conservation equation, Darcy's law, and an equation of

0021-9991/93 $5.00

state. Mass conservation in a porous medium with porosity φ is written

$$\partial_t'(\varphi\rho) + \partial_i'(\rho q_i) = 0, \tag{1}$$

where ρ is the fluid density and q_i are the components of the Darcy velocity. Considering a diagonal permeability tensor with three components K_1, K_2, and K_3, and denoting the acceleration due to gravity by g, the viscosity by μ, and the pressure by p, Darcy's law can be written

$$\begin{aligned} q_1 &= -\mu^{-1}K_1\partial_1' p, \\ q_2 &= -\mu^{-1}K_2(\partial_2' p + \rho g), \\ q_3 &= -\mu^{-1}K_3\partial_3' p. \end{aligned} \tag{2}$$

Introducing $\sigma = \varphi\rho$, $v_i = q_i/\varphi$, and the total compressibility $\beta = \sigma^{-1}\, d\sigma/dp$, and following the derivation outlined in [4], one finds that σ obeys

$$\begin{aligned} &\frac{\partial\sigma}{\partial t'} - \frac{\partial}{\partial x_1'}\left[\frac{K_1}{\varphi\mu\beta}\frac{\partial\sigma}{\partial x_1'}\right] \\ &\quad - \frac{\partial}{\partial x_2'}\left[\frac{K_2}{\varphi\mu\beta}\frac{\partial\sigma}{\partial x_2'} + \frac{K_2 g}{\varphi^2\mu}\sigma^2\right] \\ &\quad - \frac{\partial}{\partial x_3'}\left[\frac{K_3}{\varphi\mu\beta}\frac{\partial\sigma}{\partial x_3'}\right] = 0. \end{aligned} \tag{3}$$

It is shown in [4] that a lattice gas exists, such that its density satisfies Eq. (3) with constant coefficients and with $K_1 = K_3$. It is shown below that a slight generalization of the assumptions of [4] allows simulation of Eq. (3) as it stands.

3. THE LATTICE GAS MODEL

The essential ingredients of the lattice gas model have been presented in [4]. They are repeated here for completeness, together with the necessary generalizations.

The lattice is square for the two-dimensional model, with four possible directions for particle movement, indicated, as in [4], by the four unit vectors $\mathbf{e}_1, \ldots, \mathbf{e}_4$. The vertical downward direction, singled out by gravity, is along $\mathbf{e}_4$. In the three-dimensional model the lattice is cubic, and the two extra directions for particle movement are indicated by $\mathbf{e}_5$ and $\mathbf{e}_6$. The unit vectors along the coordinate axes, $\mathbf{i}_1$, $\mathbf{i}_2$, and $\mathbf{i}_3$, point, respectively, along $\mathbf{e}_1$, $\mathbf{e}_2$, and $\mathbf{e}_5$. See Fig. 1.

In the interval of a time step, each particle jumps from a node to one of its nearest neighbors. The distance between two nearest nodes is denoted by λ and the duration of a time-step is denoted by τ. The magnitude of the particle velocity is then $c = \lambda/\tau$. A particle is said to be of type α if its velocity is $c\mathbf{e}_\alpha$. The dimensionality of the model is denoted by d: $d = 2$ or 3.

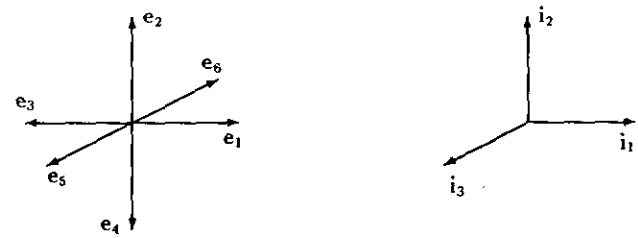

FIG. 1. The velocity directions (left) and the coordinate axes (right).

Three types of coordinates will be used in the sequel: (x_1', x_2', x_3', t') have dimensions of length and time; (x_1, x_2, x_3, t) are dimensionless, with a special scaling aimed at the perturbation expansion of the lattice Boltzmann equations; finally $(\xi_1, \xi_2, \xi_3, \theta)$ are dimensionless, with λ and τ taken as units of length and time.

The rules for particle movement are as follows (see Fig. 2):

1. At a given node and at a given time-step, not more than one particle can be found with a given type. There are thus at most $2d$ particles at a node.

2. A particle which is alone at a node at time t', is at one of the $2d$ nearest nodes at time $t' + \tau$, with a velocity pointing away from the node it just left. Transitions occur with given probabilities: there is a probability $p_{\alpha\beta}$ that a particle which is of type α at t' is of type β at $t' + \tau$.

3. If there is more than one particle at a node at time t' then, at time $t' + \tau$, each particle has jumped to the nearest node in the direction of its time-t' velocity (no collisions), except in the following situation: if there are exactly two particles at a node at t', and one of them is of type 2, then

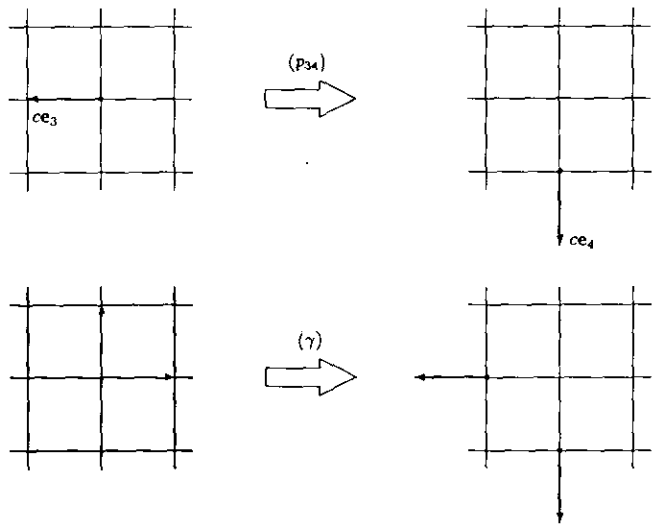

FIG. 2. Illustrations of the rules governing particle movements. Directions $\mathbf{e}_5$ and $\mathbf{e}_6$ are not shown. Time is t' ($t' + \tau$) for the diagrams at the left (right). The symbols in parentheses give the probabilities for the shown transitions to take place.

at $t'+\tau$ the probability is γ that each particle has jumped to the nearest node in the direction opposite to its time-t' velocity (and the probability is $1-\gamma$ that each particle has jumped to the nearest node in the direction of its time-t' velocity).

The accomodation of boundary conditions, and the simulation of sources and sinks, require special handling [4].

Referring to [4] for details, the following statements can now be made. As a consequence of the fact that the above rules conserve particle number but not particle momentum, the lattice gas has just one, scalar, equation of motion. Rule 2 gives rise to diffusion and rule 3 to the effect of gravity with the required form, i.e., quadratic in the density (see Eq. (3)). The particular choices made for γ and for the $p_{\alpha\beta}$ determine the magnitude of the numerical coefficients in the equation of motion, and all cases of practical interest can be accomodated by a special set of simple formulas for the $p_{\alpha\beta}$. The probability matrix must satisfy

$$\begin{aligned} &\sum_{\beta=1}^{2d} p_{\alpha\beta}=1 \qquad (\alpha=1,\ldots,2d),\\ &\sum_{\alpha=1}^{2d} p_{\alpha\beta}=1 \qquad (\beta=1,\ldots,2d). \end{aligned} \tag{4}$$

Finally, the matrix with elements $p_{\alpha\beta}-\delta_{\alpha\beta}$, where $\delta_{\alpha\beta}$ is the Kronecker delta, must be of rank $2d-1$. This condition is imposed by the necessity of eliminating the possibility of spurious conservation laws [1, 4].

Two generalizations are introduced here, relatively to [4]. The first generalization concerns the matrix $(p_{\alpha\beta})$ and is aimed at simulating a diagonal permeability tensor with three distinct components. This matrix is now written:

$$(p_{\alpha\beta})=\begin{pmatrix} F_1 & \bar\omega & B_1 & \bar\omega & \bar\omega & \bar\omega\\ \bar\omega & F_2 & \bar\omega & B_2 & \bar\omega & \bar\omega\\ B_1 & \bar\omega & F_1 & \bar\omega & \bar\omega & \bar\omega\\ \bar\omega & B_2 & \bar\omega & F_2 & \bar\omega & \bar\omega\\ \bar\omega & \bar\omega & \bar\omega & \bar\omega & F_3 & B_3\\ \bar\omega & \bar\omega & \bar\omega & \bar\omega & B_3 & F_3 \end{pmatrix}, \tag{5}$$

where

$$\begin{aligned} &F_i=(1+\delta_i)/2-(d-1)\bar\omega,\\ &B_i=(1-\delta_i)/2-(d-1)\bar\omega, \qquad i=1,2,3. \end{aligned} \tag{6}$$

For the two-dimensional model ($d=2$), the last two columns and the last two lines in matrix (5) are dropped. For an interpretation of the δ_i and $\bar\omega$ see [4].

The requirement that the elements of the matrix (5) be real numbers between 0 and 1 implies the following constraints on the δ_i and $\bar\omega$:

$$0\leqslant|\delta_i|<1 \qquad (i=1,2,3), \tag{7}$$

$$\begin{aligned} &0<\bar\omega\leqslant(1-\delta_m)/(2(d-1)),\\ &\delta_m=\max\{|\delta_1|,|\delta_2|,|\delta_3|\}. \end{aligned} \tag{8}$$

The strict inequalities—to the right for δ_i and to the left for $\bar\omega$—are imposed by the additional requirement that the matrix with elements $p_{\alpha\beta}-\delta_{\alpha\beta}$ be of rank $2d-1$.

The second generalization, aimed at simulating inhomogeneity, is obtained by assuming that parameters δ_i, $\bar\omega$, and γ are space dependent.

4. THE BOLTZMANN EQUATIONS AND THEIR PERTURBATION SOLUTION

Let $f_\alpha(\mathbf{r}', t')$ be the probability of finding a particle at node $\mathbf{r}'$ and time t', with velocity direction $\mathbf{e}_\alpha$. The evolution of f_α is given by

$$f_\alpha(\mathbf{r}'+\lambda\mathbf{e}_\alpha, t'+\tau)-f_\alpha(\mathbf{r}', t')=\Omega_\alpha, \tag{9}$$

where the collision term Ω_α can be found from the rules of Section 3 governing particle movement. To find Ω_α one uses Boltzmann's assumption of molecular chaos so that many-particle distribution functions are expressed as products of the one-particle distribution functions f_α. The detailed expressions of the Ω_α ($\alpha=1,\ldots,2d$) are given in [4]. The Ω_α are linear functions of the probabilities $p_{\alpha\beta}$ and γ, the coefficients being nonlinear expressions of the f_α. Due to the local character of the rules of particle movement, the Ω_α do not depend on the derivatives of the f_α. Due to the particle conserving property of these rules, the Ω_α satisfy

$$\sum_{\alpha=1}^{2d}\Omega_\alpha=0. \tag{10}$$

A differential version of the lattice Boltzmann equations (9) is produced by assuming that the f_α are infinitely smooth and have appreciable variations over lengths $L\gg\lambda$ and time-intervals $T\gg\tau$. The ratio

$$\lambda/L\equiv\varepsilon\ll 1 \tag{11}$$

is chosen as the small parameter which will eventually rule the perturbation expansion and one assumes [1, 4] that

$$\tau/T=\varepsilon^2. \tag{12}$$

Introducing dimensionless space and time coordinates

$$x_i=x_i'/L, \qquad t=t'/T, \tag{13}$$

one then finds that the differential version of Eq. (9) is

$$\sum_{n=1}^{\infty} \frac{1}{n!} (\varepsilon^2 \partial_t + \varepsilon e_{\alpha i} \partial_i)^n f_\alpha(\mathbf{r}, t) = \Omega_\alpha(f_\alpha). \tag{14}$$

The connection with hydrodynamics is made by defining the lattice gas density ρ by

$$\rho(\mathbf{r}, t) = \sum_{\alpha=1}^{2d} f_\alpha(\mathbf{r}, t). \tag{15}$$

As mentioned in the Introduction, the model assumes that the density is low. Specifically, this is done by setting

$$\rho(\mathbf{r}, t) = 2d\varepsilon\phi(\mathbf{r}, t), \tag{16}$$

where ε is defined by Eq. (11). The factor $2d$ is included for later convenience.

The equations of motion of the lattice gas are found by a technique which is outlined, in its essential characteristics, in [1]. In the present case, the technique is based on the application of regular perturbation theory to Eqs. (14), starting with the assumption that the solutions f_α of these equations can be found as expansions in powers of ε. It is shown in [4] that the correct form for this expansion is

$$f_\alpha = \varepsilon\phi + \varepsilon^2 f_\alpha^{(2)} + \varepsilon^3 f_\alpha^{(3)} + \cdots, \tag{17}$$

where the $f_\alpha^{(a)}$ obey

$$\sum_{\alpha=1}^{2d} f_\alpha^{(a)} = 0, \qquad a = 2, 3, \ldots, \tag{18}$$

so that the substitution of Eqs. (17) in Eq. (15) yields Eq. (16). An ingredient of the perturbation technique described in [1] is the so-called multiple-time formalism. One assumes the existence of a succession of time scales with a collective mode—and consequently an equation of motion—corresponding to each time scale. One assumes, in effect, that the f_α depend on times $t_2 = t$, $t_3 = \varepsilon t$, ...: $f_\alpha(\mathbf{r}, t_2, t_3, \ldots)$. This means that the differential time operator in Eq. (14) can be written

$$\varepsilon^2 \partial_t = \varepsilon^2 \partial_{t_2} + \varepsilon^3 \partial_{t_3} + \cdots. \tag{19}$$

Only the first time scale (t_2) and its collective mode were considered in [4]. In the present paper, the second time scale (t_3) and its collective mode will be considered as well. Some indications about the third time scale will also be given. The perturbation technique proceeds now as in the familiar regular perturbation theory. One uses Eqs. (17) and (19) in Eqs. (14) and expands both sides of these equations in powers of ε. This results in expressions of the type

$$\sum_{n=1}^{\infty} \frac{1}{n!} (\varepsilon^2 \partial_t + \varepsilon e_{\alpha i} \partial_i)^n f_\alpha(\mathbf{r}, t) = \varepsilon^2 D_\alpha^{(2)}(\phi) + \varepsilon^3 D_\alpha^{(3)}(\phi, f_\alpha^{(2)}) + \varepsilon^4 D_\alpha^{(4)}(\phi, f_\alpha^{(2)}, f_\alpha^{(3)}) + \cdots, \tag{20}$$

$$\Omega_\alpha(f_\alpha) = \varepsilon^2 \Omega_\alpha^{(2)}(\phi, f_\alpha^{(2)}) + \varepsilon^3 \Omega_\alpha^{(3)}(\phi, f_\alpha^{(2)}, f_\alpha^{(3)}) + \cdots, \tag{21}$$

where, as a consequence of Eq. (10),

$$\sum_{\alpha=1}^{2d} \Omega_\alpha^{(a)} = 0 \qquad (a = 2, 3, \ldots). \tag{22}$$

Detailed expressions for the $\Omega_\alpha^{(a)}$ ($a = 2, 3$) and for the $D_\alpha^{(a)}$ ($a = 2, 3, 4$) are given in [5]. The equality of the right-hand sides of Eqs. (20) and (21) is obtained by equating the coefficients of the corresponding powers of ε. This gives the $f_\alpha^{(2)}$ and $f_\alpha^{(3)}$ in terms of ϕ. Specifically, the $f_\alpha^{(2)}$ are obtained by solving

$$\Omega_\alpha^{(2)}(\phi, f_\alpha^{(2)}) = D_\alpha^{(2)}(\phi) \qquad (\alpha = 1, \ldots, 2d-1), \qquad \sum_{\alpha=1}^{2d} f_\alpha^{(2)} = 0. \tag{23}$$

The $\Omega_1^{(2)}, \ldots, \Omega_{2d}^{(2)}$ are not independent, according to Eqs. (22). Actually, only $2d-1$ of them are independent, so that the $f_\alpha^{(2)}$ can be made to satisfy the constraining equations (18) which are incorporated in the set of Eqs. (23). Further, Eqs. (22) imply the condition for the computability of the $f_\alpha^{(2)}$,

$$\sum_{\alpha=1}^{2d} D_\alpha^{(2)}(\phi) = 0,$$

which, according to the expressions given in [5], is identically satisfied. In the same way, the $f_\alpha^{(3)}$ are obtained by solving

$$\Omega_\alpha^{(3)}(\phi, f_\alpha^{(2)}, f_\alpha^{(3)}) = D_\alpha^{(3)}(\phi, f_\alpha^{(2)}) \qquad (\alpha = 1, \ldots, 2d-1), \qquad \sum_{\alpha=1}^{2d} f_\alpha^{(3)} = 0, \tag{24}$$

and the computability condition is

$$\sum_{\alpha=1}^{2d} D_\alpha^{(3)}(\phi, f_\alpha^{(2)}) = 0. \tag{25}$$

It can be seen that, as a general rule, the computability condition of the $f_\alpha^{(a)}$ involves $f_\alpha^{(a-1)}$, $f_\alpha^{(a-2)}$, ..., $f_\alpha^{(2)}$, ϕ. Thus,

having obtained the $f_\alpha^{(3)}$, one can write the computability condition of the $f_\alpha^{(4)}$, namely,

$$\sum_{\alpha=1}^{2d} D_\alpha^{(4)}(\phi, f_\alpha^{(2)}, f_\alpha^{(3)}) = 0. \tag{26}$$

The last two computability conditions, Eqs. (25) and (26), are the equations of mass diffusion at time scales t_2 and t_3, respectively [1]. Using the expressions in [5] one finds that the two computability conditions are of the form

$$\partial_{t_2}\phi + S_2(\phi) = 0, \tag{27}$$

$$\partial_{t_3}\phi + S_3(\phi) = 0, \tag{28}$$

where S_2 and S_3 are differential operators in the space variables. The flow equation up to order ε^3 is now obtained as a differential equation in terms of the original time-variable t, by multiplying Eqs. (27) and (28) by ε^2 and ε^3 respectively, adding, and using relation (19). It is appropriate, at this point, to return to the actual particle density ρ (Eq. (16)) and to introduce lattice space- and time-variables by

$$\begin{aligned} \xi_i &= x_i'/\lambda = x_i/\varepsilon, \\ \theta &= t'/\tau = t/\varepsilon^2. \end{aligned} \tag{29}$$

The differential equation for ρ is then

$$\frac{\partial\rho}{\partial\theta} - \frac{\partial}{\partial\xi_1}\left(D_1\frac{\partial\rho}{\partial\xi_1}\right) - \frac{\partial}{\partial\xi_2}\left(D_2\frac{\partial\rho}{\partial\xi_2} + G\rho^2\right) - (d-2)\frac{\partial}{\partial\xi_3}\left(D_3\frac{\partial\rho}{\partial\xi_3}\right) = 0, \tag{30}$$

where $d = 2$ or 3, and

$$D_i = \frac{1}{2d}\frac{1+\delta_i}{1-\delta_i} + \frac{1}{d^2}\left(\frac{d-1}{1-\delta_i} - \frac{v_i\gamma}{(1-\delta_i)^2}\right)\rho \qquad (v_1 = v_3 = 1,\ v_2 = d-1), \tag{31}$$

$$G = \frac{(d-1)\gamma}{d^2(1-\delta_2)} - \frac{(d-1)^2\gamma^2}{d^3(1-\delta_2)^2}\rho.$$

One concludes from the above derivation that, to lowest and next-to-lowest order in the expansion of the Boltzmann equations, the lattice gas defined by the rules of Section 3 obeys a flow equation which is similar to the equation of one-phase flow in a porous medium, Eq. (3), provided the density ρ is small enough that the corrections of order ρ in the D_i and G coefficients can be neglected. These coefficients (with $\rho = 0$) can be made to fit the values of the corresponding coefficients in Eq. (3) by proper choices for the elements of the probability matrix (5). Note that the probability for transverse scattering, $\bar{\omega}$, is "unobservable": it does not appear in the coefficients of Eq. (30) and can be chosen arbitrarily within the limitations of inequalities (8).

Setting $\rho = 0$ in Eqs. (31), one recovers the coefficients found in [4], provided one accounts for the fact that the flow equation in [4] is written for the ϕ of Eq. (16), with variables x_i and t of Eqs. (29). Thus the corrections brought about by the next-to-lowest order conserve the essential character of the flow equation, their effect being restricted to a modification of the coefficients of diffusion and gravity by extra terms proportional to the particle density. However, if one continues the perturbation expansion of the Boltzmann equations to order ε^5, one finds a flow equation that is no longer of the same type as Eq. (3). Calculations performed with $\gamma = 0$ and $d = 2$, show that the flow equation then contains, in addition to terms which can be taken to be corrections of order ρ^2 to D_1 and D_2, the following fourth-order derivatives: $\partial^4\rho/\partial\xi_1^4$, $\partial^4\rho/\partial\xi_2^4$, and $\partial^4\rho/\partial\xi_1^2\partial\xi_2^2$. Thus the exact equation of motion of the lattice gas has, when compared to Eq. (30), an additional differential operator $\mathscr{D}(\rho)$ on the left-hand side. $\mathscr{D}(\rho)$ is due to the sum of contributions of order ε^5 and higher, in the perturbation expansion of the Boltzmann equations.

5. A NUMERICAL EXAMPLE

Given the essential assumption of small densities, embodied in Eq. (16), the purpose of the present section is to examine the deviations attached to numerical values obtained with necessarily finite lattice densities. Specifically, letting ρ_0 be a scale for the particle density of the lattice gas in a particular calculation, one aims at an estimation of the order of magnitude of the associated deviations which are, a priori, expected to be of the order of magnitude of ρ_0. To attain this aim, the results of the model are compared to a known, exact solution. This solution is described in Section 5.1. The lattice gas setup for the numerical calculation is described in Section 5.2, where the results of the calculation are also given. The comparison of the numerical results with the exact solution and the evaluation of the deviations are found in Section 5.3.

5.1. *An analytical solution*

The full equation (30) has no known analytical solution and one must turn to particular cases of this equation. Philip [6] has given a solution in two dimensions to the equation

$$\nabla(K\nabla\Phi) = 0, \tag{32}$$

where

$$K(X, Y) = 1 - 2a\cos(2\pi X)\cos(2\pi Y) + a^2\cos^2(2\pi Y) \tag{33}$$

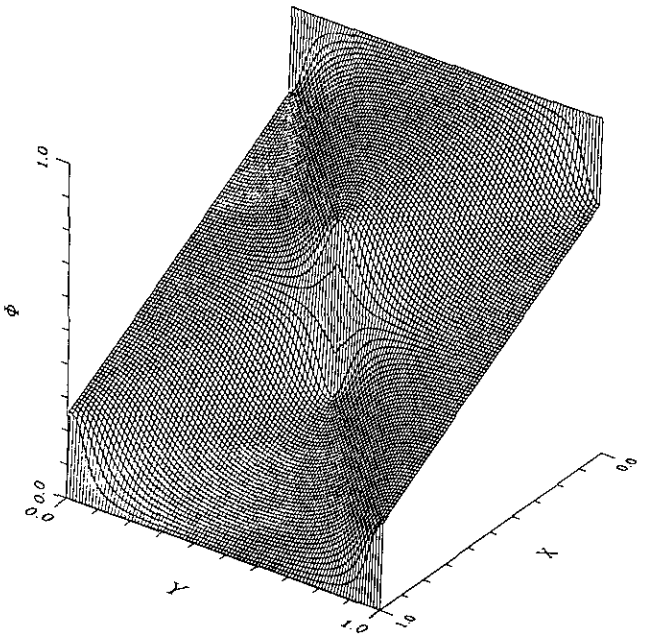

FIG. 3. The solution of Eqs. (32) and (33) when $a = 1$.

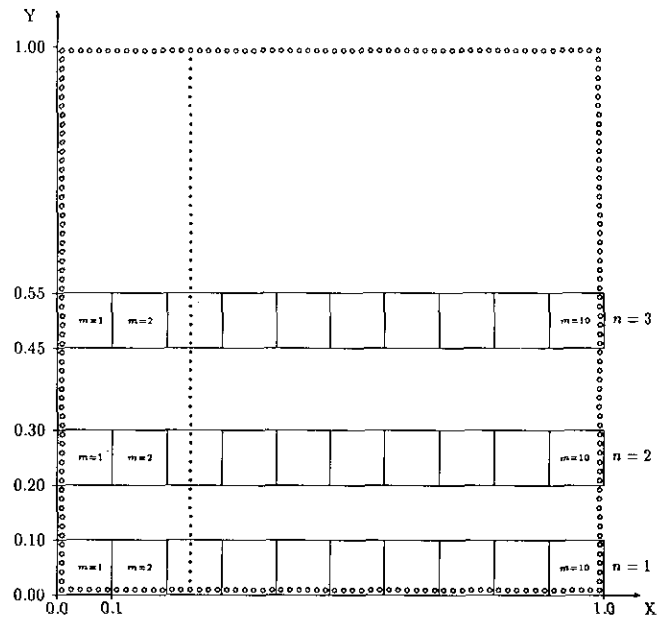

FIG. 4. Lattice for the numerical solution of Eqs. (32) and (33). The region $\{0 \leqslant X, Y \leqslant 1\}$ is covered by an $N \times N$ lattice (the figure is drawn with $N = 60$). Circles are boundary nodes, dots are ordinary nodes. Only one column of ordinary nodes is shown. The square regions making up the three horizontal stripes (ten regions per stripe) are averaging regions. See Section 5.2 for details. Referring to Eq. (30), ξ_1 and ξ_2 are along X and Y, respectively.

$(0 \leqslant a \leqslant 1$ arbitrary), in the region $\{0 \leqslant X, Y \leqslant 1\}$, with the following boundary conditions: homogeneous Neumann (no flow) at $Y = 0$ and 1, $\Phi = 1$ at $X = 0$, and $\Phi = 0$ at $X = 1$. When $a = 1$, Φ is discontinuous at the corners and at the center of the region of definition, i.e., at the same points where K vanishes. The solution for this value of a is shown on Fig. 3 (for closed-form expressions, see [6]). For the rest of this paper, $a = 1$.

5.2. *A lattice gas setup*

Equations (32), (33), and their boundary conditions, are solved numerically by first setting up a lattice to cover the region of definition (see Fig. 4). The lattice nodes are located at points (X_j, Y_k) where, say,

$$X_j = \frac{1}{N}\left(j - \frac{1}{2}\right), \qquad Y_k = \frac{1}{N}\left(k - \frac{1}{2}\right) \qquad (j, k = 1, \ldots, N).$$

The function $K(X, Y)$ is discretized as $K_{jk} = K(X_j, Y_k)$. $K(X, Y)$ is doubly periodic, with smallest period equal to $\frac{1}{2}$ and, according to the sampling theorem [3], the set of K_{jk}-values will represent $K(X, Y)$ uniquely if the sampling frequency is larger than 8π. This condition will always be satisfied since the N-values used in practical applications will always be larger than about 100.

The internal parameters of the lattice gas—essentially γ and the group $(\delta_1, \delta_2, \bar{\omega})$ determining the elements of the scattering matrix (5)—are chosen so that the coefficients of Eq. (30) match those of Eq. (32), i.e., $G = 0$ and $D_1 = D_2 = K$. Using Eqs. (31), where the ρ-corrections are assumed negligible, one easily finds that $\gamma = 0$, while $\delta_1 = \delta_2 \equiv \delta$, where δ is discretized as

$$\delta_{jk} = (4K_{jk} - 1)/(4K_{jk} + 1).$$

As already mentioned, $\bar{\omega}$ is unobservable and is restricted only by the inequalities (8). The choice

$$\bar{\omega}_{jk} = (1 - |\delta_{jk}|)/4$$

follows [4].

The boundary conditions of Section 5.1 are accommodated by reflecting particles from the upper and lower boundaries, annihilating them at the right boundary, and keeping a constant density $\rho = \rho_0$ at the left boundary. (This constant value of the density at the left boundary is taken to be the scale mentioned at the beginning of Section 5.) For more details, see [4, 5]. At zero time, the lattice is empty $(\rho = 0)$.

The lattice gas is made to run until steady state is reached. The number of time-steps necessary to reach steady state is estimated by using the result [6] that the porous medium in the region $\{0 \leqslant X, Y \leqslant 1\}$ has an effective permeability $K_e = 1$. It has been shown [4] that steady state is then approximately reached after N^2 time-steps. Starting at time-step $N^2 + 1$ and for all time-steps until $N^2 + \Delta\theta_{\text{av}}$, one

records and stores the particle densities in each of the square regions in Fig. 4. These particle densities (number of particles in each region divided by the number of nodes in that region) are conveniently denoted by $\bar{\rho}(m, n, \theta)$, where m identifies the square region from left to right in each stripe and runs from 1 to 10, n identifies the stripe and runs from 1 to 3, and θ is the time-step and runs from N^2+1 to $N^2+\Delta\theta_{av}$. (θ, as defined in Eq. (29), is a continuous time-variable with the interval between time-steps as a unit. It is used here as a time-step counter to avoid the introduction of an extra symbol.) For each square region one then calculates the average and the standard deviation with the data accumulated over $\Delta\theta_{av}$ time-steps:

$$\langle\rho\rangle_{mn}=\frac{1}{\rho_0}\frac{1}{\Delta\theta_{av}}\sum_{\theta=N^2+1}^{N^2+\Delta\theta_{av}}\bar{\rho}(m, n, \theta), \tag{34}$$

$$S_{mn}=\frac{1}{\rho_0}\left[\frac{1}{\Delta\theta_{av}-1}\sum_{\theta=N^2+1}^{N^2+\Delta\theta_{av}}[\bar{\rho}(m, n, \theta)-\langle\rho\rangle_{mn}]^2\right]^{1/2},$$

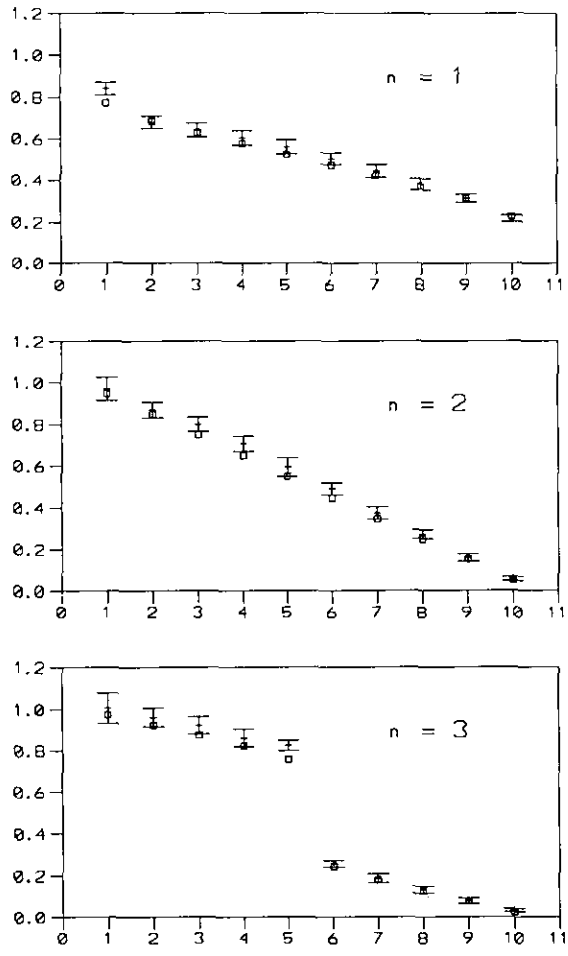

FIG. 5. Exact values (shown as open squares), and numerical results obtained with $N=600$ (shown with error bars extending one standard deviation above and one below the average value), are plotted against m, for the three values of n (see Fig. 4).

where the division by ρ_0 makes it possible to directly compare $\langle\rho\rangle_{mn}$ to $\langle\Phi\rangle_{mn}$, the average of Φ in averaging region m belonging to stripe n. As shown in Fig. 4, all averaging regions are 0.1×0.1 squares, and the three stripes have the lines $Y=0.05$, 0.25, 0.50 as axes of symmetry.

A visual comparison of $\langle\rho\rangle_{mn}$ to $\langle\Phi\rangle_{mn}$ is given in Fig. 5. The lattice gas manages the discontinuities of the solution remarkably well, considering that the premises for the derivation of the flow equation are not valid there. A quantitative comparison of the numerical results with the exact values is, in principle, straightforward. For a chosen density scale ρ_0 one would run the lattice gas model with a value of N—the lattice dimension—large enough that the standard deviations S_{mn} given in (34) are negligibly small so that the values of $\langle\rho\rangle_{mn}$ are known with the same accuracy as the values of $\langle\Phi\rangle_{mn}$. The deviations $\langle\rho\rangle_{mn}-\langle\Phi\rangle_{mn}$ would then give an indication about the accuracy of the model at that particular value of ρ_0. It is shown below that the S_{mn} are roughly proportional to $1/N$. N-values of the order of 10^4 would be necessary to make the S_{mn} appropriately small. On sequential (parallel) machines, execution time is proportional to N^4 (N^2) [4] and such large values of N are impractical. The comparison of the numerical results with the analytical values must, consequently, be made in the presence of non-negligible standard deviations S_{mn}. This is done in the next section.

5.3. *Statistical Evaluation of the Lattice gas Results*

The estimations reported here are based on the numbers which give rise to Fig. 5. In particular, $N=600$ (for tables of data at this and other values of N, see [5]). The evaluation of the $\langle\rho\rangle_{mn}$ and S_{mn} has been described in the previous section. Referring to Eq. (34), it might appear that the S_{mn} can be made arbitrarily small, regardless of lattice size N, by increasing the number of time-steps for averaging, $\Delta\theta_{av}$. This is unfortunately not the case, it is not possible to compensate for a low number of nodes in a space-averaging region by increasing the time-averaging interval. Trial runs with $N=100$ have shown that the S_{mn} slightly decrease when $\Delta\theta_{av}$ increases from 10^3 to 10^4 but remain thereafter roughly the same, even for $\Delta\theta_{av}=10^5$. All calculations reported here were made with $\Delta\theta_{av}=10^4$.

The S_{mn} will be called *errors* and it is emphasized that these are due to statistical fluctuations in particle numbers. The discrepancies between calculated and exact values, which are due to the difference between the flow equation of the lattice gas and the target differential equation (refer to the end of Section 4, starting at Eq. (30)), will be called *deviations*. The problem to be solved here is to evaluate the deviations in the presence of the errors.

A first assumption is that the contributions due to $\mathscr{D}(\rho)$ are negligible. This is not trivial, in view of the discontinuities in the exact solution (Fig. 3). However, the

contributions of $\mathscr{D}(\rho)$ are probably largest at the few discontinuities and, according to Fig. 5, are small enough to be masked by the fluctuations in the gas density. It would follow, according to Eqs. (31), that the deviations vanish with ρ. A second assumption (confirmed by more detailed calculations [5]) is that the deviations are small compared to ρ_0. Using these assumptions one can define a mean deviation d as a linear function of the density, by setting $d_{mn} = \langle\rho\rangle_{mn} - \langle\Phi\rangle_{mn}$, plotting the d_{mn} against the $\langle\rho\rangle_{mn}$, and fitting a straight line $d = a\rho + b$, where the a and b are estimated by minimizing

$$X^2 = \sum_{mn} \left(\frac{d_{mn} - a\langle\rho\rangle_{mn} - b}{S_{mn}} \right)^2.$$

Errors, Δa and Δb, on the a and b can also be calculated [2].

One finds, with the data of Fig. 5:

$$a = 0.048 \pm 0.015, \qquad b = 0.001 \pm 0.005, \qquad X^2_{\min} = 8.7.$$

The value of b is consistent with 0 and confirms that the deviations vanish with the density. The smallness of $X^2_{\min}$—minimum of X^2, and χ^2 statistic with 28 degrees of freedom—confirms that the departures from linearity, due to the contributions of $\mathscr{D}(\rho)$, are small compared to the errors due to statistical fluctuations. The size of Δa is thus mostly due to the sizes of the S_{mn}. One may conclude that the relative deviation, d/ρ, is $(5 \pm 2)\%$.

Finally, it should be mentioned that experiments carried out with the lattice gas at different values of ρ_0 and N [5] show that the standard deviations are, roughly, inversely proportional to $(N^2\rho_0)^{1/2}$, i.e., to the square root of the number of particles, a result which is familiar from Monte Carlo calculations.

6. CONCLUSIONS

The lattice gas model presented here and in [4] is a useful alternative to existing numerical methods for the numerical solution of the equation of one-phase flow in a porous medium. It can also be used to solve the heat equation and general elliptic equations of type (32). The advantages are the same as with the other lattice gas models referred to in [1], namely that of solving a specified differential equation without accumulation errors and for practically any form of boundary. In addition, the example presented here tends to show that discontinuous solutions are easily managed. The performances with less well-behaved permeabilities (small values, large gradients, discontinuities) remain to be explored. Concerning the boundary *conditions*, experience will show whether the various boundary conditions devised in relation with differential equations—Dirichlet, Neumann, and variations of those—can easily be implemented. The main disadvantage of the lattice gas model is the one shared with Monte Carlo methods: many particles are necessary to decrease the errors due to statistical fluctuations, so that large lattices are necessary. The following orders of magnitude roughly characterize the model: relative accuracies of the order of 5% should be attainable with lattice sizes of the order of 10^3 nodes per dimension and a density scale of about 0.1. Finally, concerning the practicality of the calculations, especially when it comes to computing time, it is obvious that massively parallel computers are ideally suited, although computers with vector facilities are a workable alternative in situations where results can be obtained after a moderate number of time-steps.

ACKNOWLEDGMENTS

The calculations were performed at IBM's European Petroleum Applications Center (EPAC), Stavanger. I thank R. Bratvold and K. Korsell for the invitation to use the computational facilities of the Center. I am especially grateful to Børge Rosland for much needed assistance in programming and otherwise managing the IBM 3090 (J).

REFERENCES

1. U. Frisch, D. d'Humières, B. Hasslacher, P. Lallemand, Y. Pomeau, and J.-P. Rivet, *Complex Syst.* **1**, 649 (1987).
2. A. G. Frodesen, O. Skjeggestad, and H. Tøfte, *Probability and Statistics in Particle Physics* (Universitetsforlaget, Oslo, 1979), Chaps. 10, 14.
3. A. V. Oppenheim, A. S. Willsky, and I. T. Young, *Signals and Systems* (Prentice-Hall, Englewood Cliffs, NJ, 1983).
4. P. Papatzacos, *Complex Syst.* **3**, 383 (1989).
5. P. Papatzacos, Working Papers from Rogaland University Center, 135, Stavanger 1991.
6. J. R. Philip, *Transp. Porous Media* **1**, 318 (1986).